63-3-3

Office of Naval Research
Department of the Navy
Contract Nonr-220(28)

THE COLLAPSE OF A SPHERICAL CAVITY IN A COMPRESSIBLE LIQUID

by
Robert Hickling and Milton S. Plesset

Division of Engineering and Applied Science
CALIFORNIA INSTITUTE OF TECHNOLOGY
Pasadena, California

Report No. 85-24 March, 1963

Office of Naval Research
Department of the Navy
Contract Nonr-220(28)

THE COLLAPSE OF A SPHERICAL CAVITY IN A COMPRESSIBLE LIQUID

by

Robert Hickling and Milton S. Plesset

Division of Engineering and Applied Science
California Institute of Technology
Pasadena, California

Report No. 85-24

March, 1963

THE COLLAPSE OF A SPHERICAL CAVITY IN A COMPRESSIBLE LIQUID

by

Robert Hickling and Milton S. Plesset

Abstract

This paper presents numerical solutions for the flow in the vicinity of a collapsing spherical bubble in water. The bubble is assumed to contain a small amount of gas and the solutions are taken beyond the point where the bubble reaches its minimum radius up to the stage where a pressure wave forms and propagates outwards into the liquid. The motion up to the point where the minimum radius is attained, is found by solving the equations of motion both in the Lagrangian and in the characteristic forms. These are in good agreement with each other and also with the approximate theory of Gilmore which is demonstrated to be accurate over a wide range of Mach number. The liquid flow after the minimum radius has been attained is determined from a solution of the Lagrangian equations. It is shown that an acoustic approximation is quite valid for fairly high pressures and this fact is used to determine the peak intensity of the pressure wave at a distance from the center of collapse. It is estimated in the case of typical cavitation bubbles that such intensities are sufficient to cause cavitation damage.

1. Introduction

The effect of compressibility in the collapse of a cavity in a liquid has been studied for some years. Rayleigh[1] was the first to point out that this was necessary when he showed that pressures in the liquid adjacent to the cavity wall could reach very high values. However, a real interest in the problem originated some time later, out of work on underwater explosions[2]. Analytical theories were developed by Herring[3] and Trilling[4] which were first order approximations based on Rayleigh's solution[1] for an incompressible liquid. To obtain higher order approximations the so-called Kirkwood-Bethe hypothesis[2],[5] was postulated. The Kirkwood-Bethe hypothesis forms the basis of a solution by Gilmore[6] which has been used in a modified form by Mellen[7] and by Flynn[8]. Gilmore's solution has been found to be surprisingly accurate when compared to exact solutions obtained numerically, and this behavior is again confirmed by our results.

With the advent of high-speed computers numerical solutions of the exact equations of compressible flow became possible, and several integrations of the characteristic equations have been performed. Gilmore[9] obtained some results which he used to compare with his approximate theory, while Hunter[10] performed some numerical work which acted as a basis for a similarity solution valid in the immediate neighborhood of the collapse point of an empty cavity. Brand[11] did some further computations. So far, however, there has been no numerical solution which describes the rebound of the cavity and the subsequent formation of a shock wave traveling outwards into the liquid. The work of this paper is concerned with such a solution.

Classically the problem to be solved is that of the empty cavity. This is usually quite a good model since the small amounts of gas or vapor, which occur in a typical cavitation bubble, have little effect on the motion of the interface until the final stage of the collapse. However, the contents of a cavity, even though they may be quite rarified initially, will have an important effect on the final pressure, since the further a collapse can proceed before being halted the greater the pressure. The final stage of the collapse will be affected by the behavior of the gas inside the cavity as well as by the quantity. Thus an isothermal gas can be expected to produce a more violent collapse than an equal amount of adiabatic gas. It is not our purpose in this paper to consider the physical behavior at the final collapse in detail. Such a task would in fact be quite difficult. The main interest here is in the effect of the liquid compressibility. Thus the behavior of the contents of the cavity will merely be approximated by a simple gas-like model. The cavity will be assumed to contain a uniform gas whose pressure varies according to the law $p \sim \rho^{\gamma}$, where ρ is the density. The index γ can be varied so as to simulate the gross behavior of the gas. Thus $\gamma = 1$ implies that the gas is isothermal while $\gamma > 1$ implies that some of the heat of compression is being retained in the gas. This model has the advantage of avoiding the singularities which would occur at the final collapse point if the cavity were empty. The sudden compression of a gas or vapor inside a cavity can be expected to raise its temperature, and due to conduction and condensation there will be a consequent rise in temperature in the liquid at the interface. These effects will be confined to a very narrow region[12], and they will therefore be neglected.

A sudden compression of a liquid does not cause a significant increase in temperature[13], so that it will be assumed to behave according to the well-known law $\rho^n \alpha (p+B)$ where B and n are constants. The results presented here are for water with B equal to 3,000 atmospheres and the index n equal to 7. The validity of these values has been discussed elsewhere[2], [10]. It is also assumed that the liquid is inviscid and that the motion remains spherically symmetric at all times. This description of a collapsing cavity is of course not completely accurate in detail, but it is considered to be sufficiently satisfactory for a study of the effects of liquid compression.

Numerical solutions of the equations of compressible flow for a collapsing cavity in water are presented here for both the characteristic and the Lagrangian forms of the equations. A comparison between the two provides a check on the numerical accuracy. The Lagrangian solution was carried beyond the final collapse point into the region where the liquid rebounds and generates a compression wave which travels outwards from the collapse center. The solution was terminated when the compression wave had steepened into a shock front. It could probably have been continued beyond this stage by using techniques such as those proposed by von Neumann and Richtmeyer[14] and Lax[15], where an artificial viscosity is introduced into the equations of motion to produce a continuous variation through the shock. However, enough information had already been obtained to estimate the order of magnitude of peak intensities at a distance from the collapse center so that no attempt was made to undertake this additional calculation.

One of the principal purposes of this analysis was to determine

whether shocks emanating from the collapse of cavitation bubbles could provide a mechanism for cavitation damage. The results given here show that such shocks can be strong enough to cause damage to metals and other solids in the vicinity of the bubble.

2. Formulation of the Problem

A spherical cavity containing a uniform gas is assumed to expand or contract in an infinite volume of liquid. For cavitation bubbles the effect of gravity is generally quite small, so that it will be neglected along with other asymmetric effects. Since the motion is spherically symmetric, it will be irrotational i.e.

$$\text{curl } \vec{u} = 0 \tag{1}$$

where $\vec{u}$ is the velocity vector. If the center of the bubble is chosen as the center of a system of spherical polar coordinates, then $\vec{u}$ will have only a single component u lying in the radial direction. The equations of motion expressing the conservation of mass and momentum for a spherically symmetric system are

$$\frac{D\rho}{Dt} = -\rho \left[\frac{\partial u}{\partial r} + \frac{2u}{r}\right] , \tag{2}$$

$$\rho \frac{Du}{Dt} = -\frac{\partial p}{\partial r} , \tag{3}$$

where p and ρ are the pressure and density in the liquid, and the operator

$$\frac{D}{Dt} = \frac{\partial}{\partial t} + u \frac{\partial}{\partial r} \tag{4}$$

is the derivative with respect to time following the motion of the liquid. It is assumed that the liquid is isentropic[2] and that the density and pressure are related by an equation of state of the form

$$\frac{p+B}{p_\infty+B} = \left(\frac{\rho}{\rho_\infty}\right)^n \tag{5}$$

where p_∞ and ρ_∞ are the pressure and density in the liquid at infinity. For water the constant B is given a value of 3,000 atmospheres while the index n has the value 7. The use of this equation has been justified by several authors[2], [10] and is based on the fact that entropy changes are small even when very large pressure jumps are present. The upper limit on the accuracy of the formula appears to be for pressures of about 10^5 atmospheres. The velocity of sound c in the liquid is defined by

$$c^2 = \frac{dp}{d\rho} = \frac{n(p+B)}{\rho} \quad . \tag{6}$$

The velocity of sound at infinity is therefore given by $c_\infty = [\, n(p_\infty+B)/\rho_\infty]^{\frac{1}{2}}$.

The equations of motion given above are in the Eulerian form which describes what is happening at a particular point in space and how it varies with time. However, it is preferable here to use the Lagrangian form where the properties of the fluid are obtained by following the particle motion. To do this, it is necessary to ascribe to each particle of fluid a value of a certain parameter, y, which is defined by the expression

$$y = \int_{r(o,t)}^{r(y,t)} \rho r^2 dr \quad .$$

Hence

$$\rho r^2 \frac{\partial r}{\partial y} = 1 \quad . \tag{7}$$

With this relation, Eq.(4) becomes

$$\rho r^2 \left(\frac{\partial r}{\partial y}\right)_t = 0 \tag{8}$$

but, since Eq.(7)is a solution of this equation, the two conditions are equivalent.

On the walls of the cavity the pressure is given by the relation

$$P = p_o(R_o/R)^{3\gamma} \tag{9}$$

where p_o is the initial pressure inside the cavity prior to collapse and R_o is the initial radius of the cavity. Capital letters are used to denote the values of variables at the cavity wall. Thus R is the radius of the cavity and U its velocity. At infinity the liquid is at rest and the pressure and density have the values p_∞ and ρ_∞. All that now remains before solving the equations is to specify the pressure and velocity in the liquid at some initial instant. For a cavity in an incompressible liquid, it is usual to suppose that the liquid is initially at rest and at a uniform pressure p_∞ and that the collapse is generated by a pressure discontinuity at the cavity wall i.e. $p_\infty > p_o$. The instant this pressure discontinuity is allowed to take effect, it is felt throughout the entire volume of the liquid because of the incompressibility. The cavity wall then starts to accelerate inward from rest. For a compressible liquid there would be an initial jump in velocity during an infinitesimal period of time. Gilmore[6] has shown that this instantaneous increase in velocity is

given by the relation

$$U_o = \frac{2}{(n-1)} (c_o - c_\infty) \tag{10}$$

where $c_o = [n(p_o+B)/\rho_o]^{\frac{1}{2}}$. The maximum value of p_∞ used here is 10 atmospheres, so that for water, such a jump in velocity will always be quite small compared to sonic velocities. In fact, during the early stages of the collapse, the solution will be indistinguishable from that for the incompressible liquid. Because of their simplicity the same initial conditions will be used in the present analysis and, even though it is not really necessary, the effect of the initial jump in velocity will be included. The possibility of the formation of an initial compression wave in the gas or vapor inside the cavity is neglected. The initial conditions are somewhat artificial and there is not much to be gained here in following up such an implication.

A method widely used in the solution of the equations of compressible flow is the method of characteristics. The characteristic equations for spherically symmetric flow are

$$\frac{\partial r}{\partial \alpha} = (u+c) \frac{\partial t}{\partial \alpha} , \tag{11}$$

$$\frac{\partial r}{\partial \beta} = (u-c) \frac{\partial t}{\partial \beta} , \tag{12}$$

and

$$\frac{\partial u}{\partial \alpha} + \frac{c}{\rho} \frac{\partial \rho}{\partial \alpha} + \frac{2cu}{r} \frac{\partial t}{\partial \alpha} = 0 ,$$

$$\frac{\partial u}{\partial \beta} - \frac{c}{\rho} \frac{\partial \rho}{\partial \beta} - \frac{2cu}{r} \frac{\partial t}{\partial \beta} = 0 .$$

The last two equations are not very suitable for finite difference work since ρ varies quite slowly in the liquid. Since $\delta\rho = \delta p/c^2$, the alternative forms

$$\frac{\partial u}{\partial \alpha} + \frac{1}{\rho c} \frac{\partial p}{\partial \alpha} + \frac{2cu}{r} \frac{\partial t}{\partial \alpha} = 0 \tag{13}$$

$$\frac{\partial u}{\partial \beta} - \frac{1}{\rho c} \frac{\partial p}{\partial \beta} - \frac{2cu}{r} \frac{\partial t}{\partial \beta} = 0 \tag{14}$$

are used. Equations (1 1) and (1 2) define the system of characteristic lines α and β where α is the outward-going characteristic and β the inward going. The bubble wall motion is defined by the variable ℓ and is determined from the expressions

$$\frac{\partial R}{\partial \ell} = U \frac{\partial t}{\partial \ell} \tag{15}$$

and

$$\frac{\partial \rho}{\partial \ell} = \frac{dp}{dR} \frac{\partial R}{\partial \ell} \cdot \tag{16}$$

Related to the method of characteristics is the approximate theory of Gilmore[6] which is based on the so-called Kirkwood-Bethe assumption[2]. This states that the quantity $r\left[h(p) + \frac{u^2}{2}\right]$ is a constant along an outward going characteristic, where

$$h(p) = \int_{p_\infty}^{p} \frac{dp}{\rho} = \frac{1}{(n-1)} (c^2 - c_\infty^2) \tag{17}$$

is the enthalpy difference between the liquid at pressure p and at pressure p_∞ under isentropic conditions. This assumption can be expressed in the form of an equation containing the particle derivative as defined in Eq. (4). Since the cavity wall moves with the liquid, and since this motion can be expressed purely as a function of time, such particle derivatives can be changed into ordinary derivatives with respect to time and the equation will become

$$R \frac{dU}{dt}\left[1 - \frac{U}{C}\right] + \frac{3}{2} U^2\left[1 - \frac{U}{3C}\right] = H\left[1 + \frac{U}{C}\right] + \frac{R}{C}\frac{dH}{dt}\left[1 - \frac{U}{C}\right] \tag{18}$$

which governs the motion of the cavity wall. Given the initial values on the boundary, a second ordinary differential equation gives the liquid conditions along an outward-going characteristic line:

$$\frac{du}{dt} = \frac{R(H+U^2/2)(u+c)}{r^2(c-u)} - \frac{2c^2u}{r(c-u)} \quad . \tag{19}$$

This is solved in conjunction with the Kirkwood-Bethe assumption and Eqs. (11) and (17).

For most problems of interest in bubble collapse it can be assumed that $|H| << C^2$. With water for example, this inequality corresponds to a pressure difference $|p_o - p_\infty| << 20{,}000$ atmos. Using this assumption, Gilmore[6] was able to derive a simple relation between the bubble wall velocity and the radius, for the case of an empty cavity. This relation is

$$\left[\frac{R_o}{R}\right]^3 = \left[1 - \frac{U}{3C}\right]\left[1 + \frac{3\rho_\infty U^2}{2(p_\infty - p_o)}\right] . \tag{20}$$

It is seen that as R tends to zero, U varies as $R^{-\frac{1}{2}}$, in contrast to incompressible theory[1] which gives U varying as $R^{-3/2}$.

The variables used in the above equations were non-dimensionalized with respect to the initial radius R_o, the density ρ_∞, and velocity of sound c_∞ in the following way:

$$\rho = \rho/\rho_\infty \; ; \quad p' = p/\rho_\infty c_\infty^2 \; ; \quad u' = u/c_\infty \; ;$$

$$t' = c_\infty t/R_o \; ; \; h' = h/c_\infty^2 \; ; \quad r' = r/R_o \; .$$

It will be supposed that all the variables and constants used above have already been non-dimensionalized in this way, and the primes suppressed. The equations of motion will remain unaltered by this change, but the liquid equation of state Eq. (5) becomes

$$n(p + B) = \rho^n \quad , \tag{21}$$

and the pressure at the bubble wall given by Eq. (9) becomes

$$P = p_o R^{3\gamma} \quad . \tag{22}$$

Equations (10) and (17) are modified by setting $c_\infty = 1$.

It will be seen from this non-dimensionalization that the solutions are actually independent of the initial radius R_o, i.e., that the same pressures and velocities are obtained regardless of the scale. (The elapsed time is of course proportional to R_o). This is due to the fact that compressible flow equations contain only first order derivatives. If effects such as heat-conduction, viscosity and surface tension were included, the solutions would become dependent on R_o, the dependence becoming stronger with a decrease in R_o.

Solutions to the problem of bubble collapse were obtained by means of a high-speed computer, using the three methods given above. First of all Gilmore's method was used to establish an approximate solution for the motion of the cavity wall. The initial conditions given above were applied, together with the initial value of the velocity given by Eq. (10). The validity of this solution was checked in relation to simple incompressible flow theory[1] for the early stages of the motion. Some exploratory calculations were then carried out using the method of characteristics in the region where the Mach number U/C at the cavity wall was of the order of 0.1. These results were compared, both on the wall and in the interior of the liquid, with results obtained by Gilmore's method, and it was established that the method was quite accurate in

this region. This result was of course to be expected since it can be shown [6] that Gilmore's theory is accurate to terms at least of the order of $(u/c)^2$. Thereafter, Gilmore's method was used to provide initial values in the subsonic $(U/C \sim 0.1)$ region for the solution of the Lagrangian and the characteristic equations. Such a procedure was necessary because of the large amount of computing time required to perform an exact solution starting from the initial stages of the motion. The Lagrangian and the characteristic solutions were carried to the final collapse point and, since they are both supposed to be exact, they provided a check on the numerical accuracy up to this stage. Comparisons were made for points on the cavity wall and in its vicinity, and the discrepancies which occurred were estimated to be at most about one per cent. The Lagrangian solution was then carried on into the region of rebound up to the point where a shock wave formed. Solutions were obtained for a variety of conditions such as might occur in cavitation. The values used for the ambient pressure p_∞ in the liquid were 1 atmosphere, and 10 atmospheres. The initial pressure p_o in the gas was varied from 10^{-1} atmospheres to 10^{-4} atmospheres, while the index γ for the gas had the values 1 and 1.4. The problems were programmed for an IBM 7090 and the numerical methods are described in the appendices.

3. Calculated Results

The first set of calculations were concerned with the motion of the bubble wall and with the gross effect of the gas content of the bubble. Figures 1 - 3 show the variation of the bubble wall Mach number with the radius under a variety of conditions. The amount of gas is determined

by the initial pressure p_o, and the behavior of the gas is varied by changing the index γ. Figure 1 shows the collapse of a bubble for different initial pressures p_o with $\gamma = 1.4$, acting under an external pressure p_∞ of 1 atmosphere. It is seen that as the amount of gas diminishes, the motion of the bubble wall becomes more and more rapid during the final stages of the collapse. In the case of the empty cavity, the velocity increases without limit as the bubble grows smaller. The exact solutions are compared with solutions derived from Gilmore's theory and from the theory of an empty cavity in an incompressible liquid. It is seen that the compressibility becomes very important during the final stages of the motion. Figure 2 shows the result of increasing the external pressure p_∞ from 1 atmosphere to 10 atmospheres. A comparison with Fig. 3 shows that such an increase does not affect the collapse so much as a change in γ from 1.4 to 1. Thus a gas which behaves isothermally should in general produce a more violent collapse than an adiabatic gas reacting under a high external pressure. In all these results, it is evident that the predictions of Gilmore's theory, based on the Kirkwood-Bethe assumption, continue to be surprisingly accurate.

For the empty cavity under 1 atmosphere external pressure, the bubble wall velocity tends to infinity as $(R_o/R)^{0.785}$. The value of the index was found to be the same when p_∞ was 10 atmospheres. This result is in good agreement with a similar estimate by Hunter[10]. By comparison, Gilmore's theory predicts a rate varying as $(R_o/R)^{0.5}$, while the incompressible theory gives $(R_o/R)^{1.5}$.

The remaining results are concerned with the flow in the liquid

around the collapsing bubble and were obtained for the two cases, $p_o = 10^{-3}$ and 10^{-4} atmospheres, with $\gamma = 1.4$ and an external pressure of 1 atmosphere. In both these cases the liquid rebounds and forms a compression wave which moves outwards and steepens into a shock front. The occurrence of the shock front causes the numerical solution to become unstable so that the results are only presented up to this point. Methods are available[14], [15] for overcoming this instability, and proceeding with the solution. But this continuation would have involved an additional program of computation and, since it is not really necessary for the purposes of this paper, it was not pursued. Figure 4 - 7 show the distributions of Mach number and pressure in the liquid. These are given for successive instants in time which is expressed in terms of τ, the time required for the bubble to collapse from the initial radius R_o to the final minimum radius. The formula used to determine the time scale is $(\tau - t)10^4/\tau$ where t is the time elapsed from the start of the motion. The collapse time τ was determined accurately from the numerical solutions. It can also be estimated by use of the incompressible theory for an empty cavity in an incompressible liquid. The incompressible relation gives

$$\tau \sim 0.91\, R_o(\rho_\infty/p_\infty)^{\frac{1}{2}} \quad .$$

Estimates from this agree to within less than 1% with values obtained in the calculated examples.

Figures 5(b) and 7(b) show the pressure wave forming and traveling outwards into the liquid. Because of the compressiblity, the change in the direction of motion of the interface is communicated to the liquid

nly by the passage of the pressure wave, and hence a reversal of flow occurs through it, as shown in Figs. 4 and 6. The shock wave forms fairly rapidly when the initial pressure is 10^{-4} atmospheres, because the final collapse pressures are high. In the case where the initial pressure is 10^{-3} atmospheres, the pressure front does not steepen so quickly. When $p_o = 10^{-2}$ atmospheres, the final pressure at the cavity wall is seen, from Fig. 1, to be about 10^3 atmospheres. For liquid pressures of this magnitude, the compression wave will steepen only very slowly and the rate with which it steepens is reduced as it moves outwards, because of geometric attenuation. For such cases the compression will behave like an acoustic wave, which does not alter much in form as it propagates. For larger amounts of gas inside the bubble, the intensity of the compression will diminish even further until only a very weak pulse emanates from the collapse.

Figure 5(b) shows that the acoustic approximation is reasonably valid even in the case where a shock front develops. The pressure front gradually steepens, but the wave remains of approximately the same thickness and form and attenuates as $1/r$ as it propagates outwards from the collapse center. The last stage of the calculations shows that the peak pressure in the wave is about 1,000 atmospheres at $R/R_o \sim 0.3$. Beyond this point not much change will occur due to dispersion, and the losses due to entropy changes through the shock will be negligible[2]. Hence the pressure pulse will propagate outwards like an acoustic wave, and at $R/R_o \sim 2$ the peak intensity will be of the order of two hundred atmospheres. For smaller amounts of gas, the peak pressures will be larger although they are a little more susceptible to the effects of

dispersion. Figure 7(b), for example, shows that the peak pressure still has an approximate $1/r$ dependence giving an intensity of the order of 1,000 atmospheres when $R/R_o \sim 2$. A much stronger effect, however, would result if the gas inside the bubble were to lose some of its heat of compression. Figures 1 and 3 show that if the gas is isothermal, it collapses to a much smaller radius for the same initial amount of gas when compared to the adiabatic condition. It has been shown[16] for values of $R_o < 1$ mm, that heat losses from the gas into the liquid are quite significant. For bubbles of this size therefore, a more violent collapse would occur, and pressure wave intensities of several thousand atmospheres could be expected.

4. Application of Results to the Theory of Cavitation Damage

A well-known consequence of the formation of cavitation bubbles in a liquid is the damage which can occur to adjacent solid surfaces. Such damage has been shown[17] to be largely mechanical in origin, although the precise mechanism is as yet undecided. It has been suggested for example that the damage is caused by bubbles adhering to the solid and collapsing asymmetrically in such a way that jets of liquid form and strike the surface at high speed. There is some indication[18] that such a mechanism might operate. The results of the present paper show that damage could certainly result from pressure waves originating from bubbles situated at a short distance from the surface. This would avoid the requirement that the destructive bubbles be only those which are adhering to the surface.

Compared to usual kinds of material damage, cavitation damage is very localized. Cavitation bubbles are usually of the order of 10^{-2} cm.

in size i.e. of the order of the grain size in a typical metal. Hence the attack from the cavitation bubbles will be directed towards the individual grains rather than towards a large group of them. This would imply that cavitation stresses only need to be of the order of the yield stresses of the individual crystals. In addition the fact that the damage usually results after an exposure to cavitation of a certain duration, indicates the existence of some kind of fatigue process. The cold working which has been observed[17] during the early stages of the exposure lends support to this conclusion. It can be estimated therefore that pressures of the order of two or three thousand atmospheres should be sufficient to cause most of the kinds of cavitation damage which have been observed. It is possible of course that local stress concentrations may occur due to irregularities in surface finish and grain structure and hence the original pressures need not be as high as this. However,for present purposes it is not really necessary to consider such possibilities.

The results discussed in the previous section indicate that pressure waves of the right order of intensity can occur from collapsing cavitation bubbles. Such bubbles usually contain only very small amounts of vapor and gas, and are usually less than 1 mm. in size prior to collapse. Hence the collapse process should be violent enough to produce pressure waves of the right intensity. This estimate is based on the assumption of a spherically symmetric collapse. Both the presence of the boundary and possible instability effects[19] during the final stages of the motion can upset this symmetry and presumably reduce the intensity of the resulting pressure waves. It is believed that the results for the spherical motion give a sufficiently good indication of the order of magnitude of the pressures which can occur in practice.

APPENDIX I - THE KIRKWOOD-BETHE SOLUTION

From the theory given in Section 2, the governing equation in non-dimensionalized form for the motion of the cavity wall are:

$$\frac{dU}{dt} = [H(C+U) + \frac{R}{C}\frac{dH}{dt}(C-U) - \tfrac{1}{2}U^2(3C-U)]/R(C-U) \qquad (I.1)$$

$$\frac{dR}{dt} = U \qquad (I.2)$$

$$\frac{dH}{dt} = -3\gamma PU/R[n(P+B)]^{1/n} \qquad (I.3)$$

$$P = p_o/R^{3\gamma} \qquad (I.4)$$

$$C = [n(P+B)]^{(n-1)/2n} \qquad (I.5)$$

together with the initial conditions at $t = 0$,

$$R = 1 \;\; ; \;\; P = p_o \;\; ; \;\; C = C(p_o) \;\; ;$$

$$U = \frac{2}{(n-1)}[C(p_o)-1] \;\; ; \;\; H = \frac{1}{(n-1)}[C^2(p_o)-1] \; . \qquad (I.6)$$

These equations were solved at intervals Δt by a simple step by step iterative procedure starting from the initial values Eq.(I.6). A first estimate of U at $t = \Delta t$ was obtained by substituting the initial values into Eq.(I.1). This was averaged with the initial value of U and used in Eq.(I.2)to obtain a first estimate of R at $t = \Delta t$. The values of R were then averaged in the same way as the values of U and used in Eqs.(I.4) and(I.5)to get correspondingly averaged values of P and C. The averaged values obtained so far were then used in Eq.(I.3)to obtain an

averaged form of dH/dt and a first estimate of H at $t = \Delta t$. This procedure was repeated step by step for each interval Δt. In approaching the collapse point, the variation with time becomes quite rapid, and it is necessary to keep reducing the interval Δt in order to preserve accuracy. This was done by repeatedly carrying the solution up to the point where U becomes positive, then returning to a suitable earlier point and repeating the last stages of the calculation for a new interval $\Delta t/5$, where Δt was the previous interval.

The solution for the motion of the cavity wall provides the initial values for the following set of equations, which can be solved along an out-going characteristic in the interior of the liquid,

$$\frac{du}{dt} = \left[\frac{(c+u)}{r} Y - 2c^2u\right] / r(c-u) \qquad (I.7)$$

$$\frac{dp}{dt} = [n(p+B)]^{1/n} \left[4c^2u^2 - \frac{(c+u)^2}{r} Y\right] / r(c-u) \qquad (I.8)$$

$$\frac{dr}{dt} = (u+c) \qquad (I.9)$$

$$C = [n(p+B)]^{(n-1)/2n} . \qquad (I.10)$$

The constant Y is derived from the initial conditions and is given by

$$Y = R(H+U^2/2) \qquad (I.11)$$

where R, H, U are values on the cavity wall. This set of equations was solved in the manner already described.

APPENDIX II - THE SOLUTION OF THE CHARACTERISTIC EQUATIONS

The non-dimensionalized equations for the characteristic solution are

$$\frac{\partial r}{\partial \alpha} = (u+c)\ \frac{\partial t}{\partial \alpha} \tag{II.1}$$

$$\frac{\partial r}{\partial \beta} = (u-c)\ \frac{\partial t}{\partial B} \tag{II.2}$$

$$\frac{\partial u}{\partial \alpha} + \frac{1}{\rho c}\ \frac{\partial p}{\partial \alpha} + \frac{2cu}{r}\ \frac{\partial t}{\partial \alpha} = 0 \tag{II.3}$$

$$\frac{\partial u}{\partial \beta} - \frac{1}{\rho c}\ \frac{\partial p}{\partial \beta} - \frac{2cu}{r}\ \frac{\partial t}{\partial \beta} = 0 \tag{II.4}$$

with

$$\rho^n = n(n+B) \tag{II.5}$$

$$c = [n(p+B)]^{(n-1)/2n} \tag{II.6}$$

The method used to solve this system is the one used by Gilmore[6] and later by Brand[11]. The initial points lie along an out-going characteristic line α, with the analytic continuation being provided at the intersection with the boundary by the conditions

$$\frac{\partial R}{\partial \rho} = U\ \frac{\partial t}{\partial I} \tag{II.7}$$

$$\frac{\partial p}{\partial I} = -\ \frac{3\gamma p}{R}\ \frac{\partial R}{\partial I}\ . \tag{II.8}$$

This is somewhat shorter than the method used by Hunter[10] who took the initial values to lie along a line t = const. In the present calculations, the initial values were provided by Gilmore's method.

The Eqs.(II.1 - II.4)and(II.7)(II.8)were expressed in finite difference form and applied according to the scheme shown in Fig. 8. The initial line of points along an out-going characteristic are designated by the letter i. The point (i,j) represents the jth point on this line starting from the point on the boundary. The continuation is provided at the boundary at the intersection of the inward-going characteristic through (i, 2) with the boundary. This yields the new point (i + 1, 1). The outward-going characteristic through this new point and the inward-going characteristic through the point (i, 3) intersect at the next new point (i + 1, 2). By repeating this process, one obtains all the new points on the line (i+1). It is seen that the total number of these points is diminished by 1 compared with the line i. The kind of averaging technique described in the previous appendix was also used here to improve the accuracy.

The fact that one point was lost at each step of the solution proved to be a problem, because it was difficult to decide how many points would be needed to carry the solution to the final stages of the collapse. This was remedied by adding one point at each step using Gilmore's method. This was always done when the Mach number was small so that the new point could be considered to have an accuracy corresponding to the other points on the characteristic line. As the solution approached the last stages of the collapse, the outward-going characteristics began to extend into the region of rebound i.e. into the region $t > \tau$ where τ is the time of collapse. The main criterion for this was the time when the velocity began to turn positive at the end of the line of points. Whenever this occurred, the affected points were discarded. In this way only the

points needed to give a solution up to the final stages of collapse were preserved.

The number of points used was also determined by the motion of the bubble wall. When the collapse becomes more rapid, more points are needed to ensure the proper accuracy. As a check the first and final estimates of the velocity and pressure were compared at each step and, if these differed by a certain percentage, then an interpolation automatically occurred which doubled the total number of points. The additional points were situated at the half intervals.

The techniques described here were tested for a variety of examples, and the accuracy of the results presented is considered to be quite satisfactory. The calculations were performed on an IBM 7090 and each example took about ten minutes.

APPENDIX III - SOLUTION OF THE LAGRANGIAN EQUATIONS

The governing equations for the Lagrangian form of the solution are,

$$\rho r^2 \frac{\partial r}{\partial y} = 1 \qquad \text{(III. 1)}$$

$$\frac{\partial u}{\partial t} = -r^2 \frac{\partial p}{\partial y} \qquad \text{(III. 2)}$$

$$\frac{\partial r}{\partial t} = u \qquad \text{(III. 3)}$$

with

$$\rho^n = n(p+B) \qquad \text{(III. 4)}$$

$$c = [n(p+B)]^{(n-1)/2n} \; . \qquad \text{(III. 5)}$$

This set of equations is sufficient to determine the variables. Equation (III. 1) can be used to find ρ, whence Eq. (III. 4) yields p. However this is not a very satisfactory process, since ρ varies comparatively slowly and is not very suitable as a running variable. Hence instead of Eq. (III. 1) the following relation was used,

$$\frac{\partial p}{\partial t} = - [n(p+B)] \left[\rho r^2 \frac{\partial u}{\partial y} + \frac{2u}{r} \right] \; . \qquad \text{(III. 6)}$$

In addition the pressure on the boundary was given by

$$P = p_o / R^{3\gamma} \qquad \text{(III. 7)}$$

The above set of equations were expressed as finite differences. The variables were situated at different points in the finite difference

lattice so that the derivatives could be expressed in a different form accurate to second order. The arrangement used is shown in Fig. 9. The velocity u was evaluated at the points $(i, j + \frac{1}{2})$, the pressure p at the points $(i + \frac{1}{2}, j)$, and the radial distance r at the points $(i + \frac{1}{2}, j + \frac{1}{2})$, where i, j are the coordinates of a typical point of the lattice. At the boundary the velocity increment was found using a three point difference formula for the derivative $\partial p/\partial y$. An iteration scheme using averaged values was employed, in a manner similar to that described in the previous appendices.

The initial points were obtained using Gilmore's theory. Given a set of points describing the motion of the bubble wall, solutions are found along the outward-going characteristics starting from each of the given points and finishing on a certain line t = const. The points along this line then provide the initial points for the calculation. The increment in y between each of the points is found from Eq.(III.1).

Because of the purposes of the calculation, the computations had to be performed over a fairly extensive range of y. However, the need for accuracy decreases in moving away from the bubble wall, and the spacing of the points can be reduced correspondingly. This is already achieved to some extent by the initial points since their spacing with respect to y varies roughly as r^2. Finer accuracy is required near the boundary when the collapse becomes more rapid. Hence a scheme of interpolation was embarked on, similar to that described in Appendix II for the method of characteristics. When the differences between first and second estimates at the boundary become greater than a certain percentage, interpolations are made between the first

twenty-five points closest to the boundary. The total number of points is thereby increased with each interpolation. In order to prevent the loss at each step in time of the point farthest from the bubble wall, an extrapolation is made assuming the liquid to be incompressible. This assumption is justified because the magnitude of the velocity and pressure in this region is small. The increment in time was determined from the well-known Courant-Levy condition on the relation between sound speed and mesh speed.

The solutions were carried up to the final collapse point and beyond into the region of rebound, where a compression wave forms and moves outwards, eventually turning into a shock front. Beyond this stage the solution could presumably have been carried on using methods such as those of von Neumann and Richtmeyer[14] or Lax[15] where an artificial viscosity term is introduced into the equations of motion to create a smooth transition in flow through the shock. By this means the motion of the shock could have been followed as it moved out into the liquid. This was not attempted here, however, because it was felt that enough information had already been obtained to make an order of magnitude estimate of shock strengths at a distance from the center of collapse; to have followed the solution to any extent in this way would have involved an elaborate reconstruction of the numerical procedures together with an extensive series of test calculations.

Up to the final collapse point the Lagrangian solution could be compared to that obtained from the method of characteristics. Good agreement was found once both programs had been developed and tested. For example in the results presented here the final collapse radii agree

to within less than 1%. Other comparisons showed a similar order of agreement. After the final collapse point, the Lagrangian solution showed good agreement with physical considerations. The crest of the compression wave moved with the local speed of sound, and the attenuation under conditions where dispersive effects were not strong varied approximately in inverse proportion to the distance from the center of collapse.

The calculation time for each of the examples given here was about twenty minutes.

References

[1] Lord Rayleigh, Phil. Mag., 34, 94 - 98 (1917).

[2] R. H. Cole, "Underwater Explosions", Princeton University Press (1948).

[3] C. Herring, "Theory of Pulsations of a Gas Bubble Produced by an Underwater Explosion", OSRD Report No. 236 (1941).

[4] L. Trilling, J. Appl. Phys., 23, 14 - 17 (1952).

[5] J. G. Kirkwood and H. A. Bethe, "The Pressure Wave Produced by an Underwater Explosion", OSRD Report No. 588 (1942).

[6] F. R. Gilmore, Report No. 26 - 4 Hydrodynamics Lab. California Inst. of Technology, Pasadena, Calif. (1952).

[7] R. H. Mellen, Journ. Acoust. Soc. Amer., 28, 447 - 454 (1956).

[8] H. Flynn, Technical Memo No. 38, Acoustics Research Lab., Harvard University (1957).

[9] F. R. Gilmore, Symposium on Naval Hydrodynamics National Acad. Science - Nat. Research Council, Publication No. 515 (1957).

[10] C. Hunter, Journ. Fluid Mech., 8, 241 - 263 (1960).

[11] R. S. Brand, Tech. Rept. No. 34, Division of Applied Mathematics, Brown University (1960).

[12] M.S. Plesset and S. A. Zwick, Jour. of Applied Physics, 25, 493 - 500 (1954).

[13] P. W. Bridgman, "The Physics of High Pressures" G. Bell and Sons Ltd., London (1949) p. 141.

[14] J. von Neumann and R. D. Richtmeyer, Jour. of Applied Physics, 21, 232 - 237 (1950).

[15] P. D. Lax, Comm. Pure and Applied Math., 7, 159 - 193

[16] R. Hickling, "Effects of Thermal Conduction in Sonoluminescence" Report No. 85-21, Engineering Div., California Inst. of Tech., Pasadena, Calif. (1962).

[17] M. S. Plesset and A. T. Ellis, Trans. Amer. Soc. Mech. Eng., 77, 1055 - 1064 (1955).

[18] C. F. Naude and A. T. Ellis, Rept. No. E-108.7, Hydrodynamics Lab. California Inst. of Technology, Pasadena, Calif. (1960).

[19] M. S. Plesset and T. P. Mitchell, Quarterly of Applied Math., 13, 419 - 430 (1956).

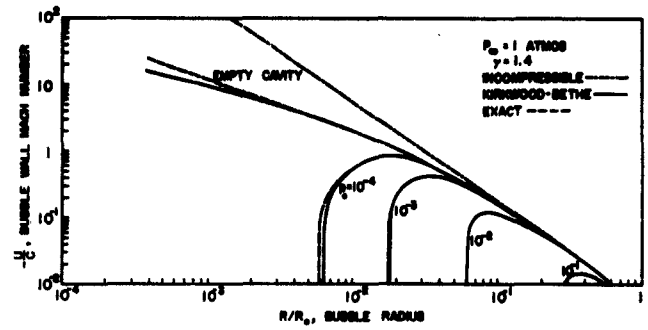

Fig. 1 The bubble wall Mach number as a function of the bubble radius for decreasing gas content. The gas content is determined by its initial pressure p_o in atmospheres. The index γ has the value 1.4 and the ambient pressure p_∞ is one atmosphere.

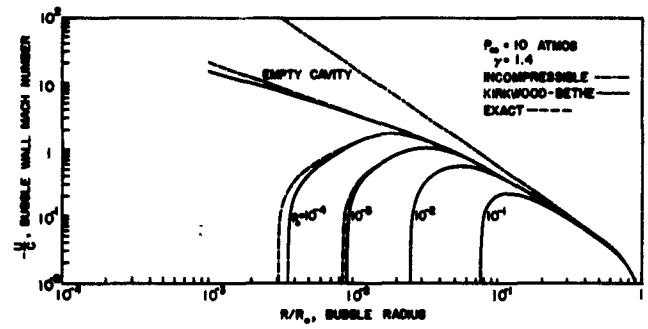

Fig. 2 The bubble wall Mach number as a function of the bubble radius for decreasing gas content. The index γ has the value 1.4 and the ambient pressure p_∞ is 10 atmospheres.

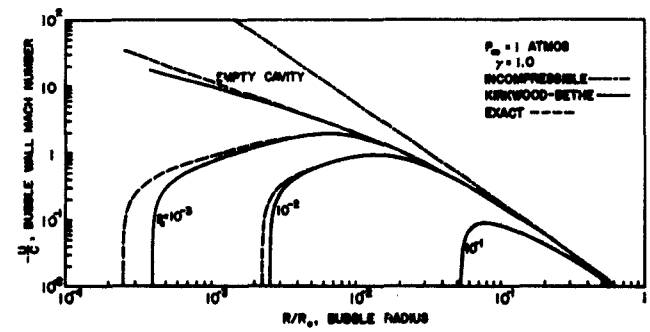

Fig. 3 The bubble wall Mach number as a function of the bubble radius for decreasing gas content. The index γ has the value 1.0 and the ambient pressure p_∞ is 1 atmosphere.

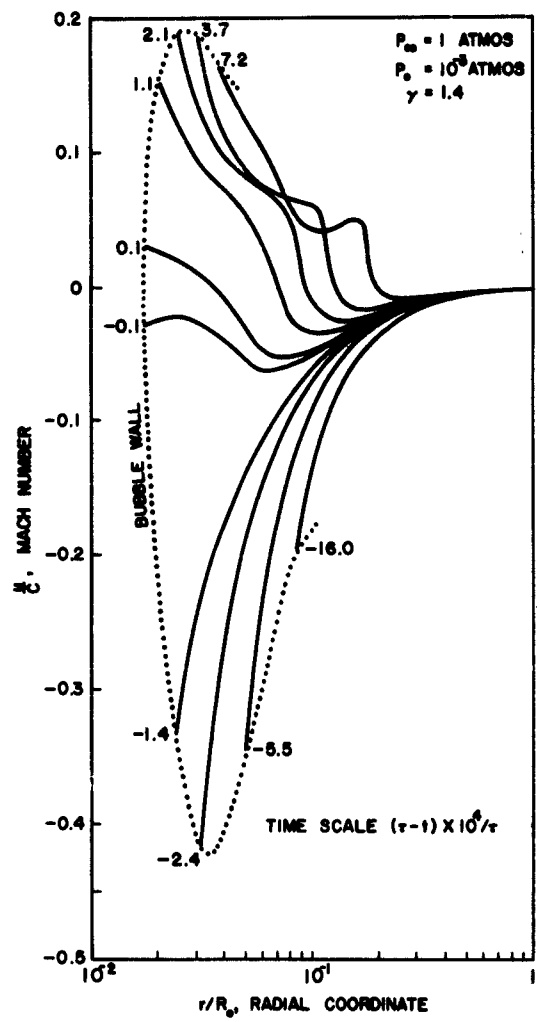

Fig. 4 Variation of Mach number with distance from the bubble wall for different instants in time during the collapse and rebound of the bubble. The initial internal pressure p_o in the gas is 10^{-3} atmospheres. The ambient pressure p_∞ is 1 atmosphere.

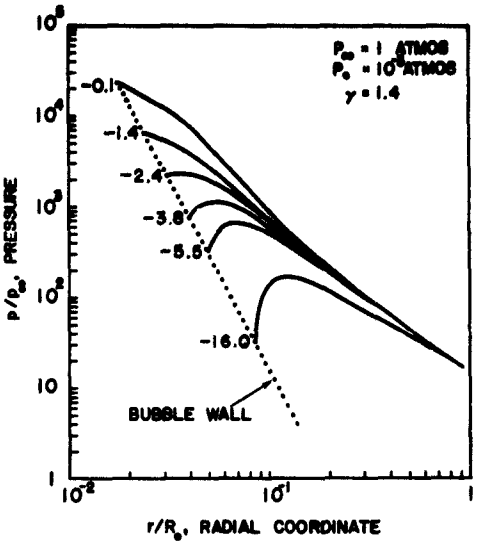

Fig. 5(a) Variation of pressure with distance from the bubble wall for different instants in time during the collapse of the bubble. The conditions correspond to those of Fig. 4.

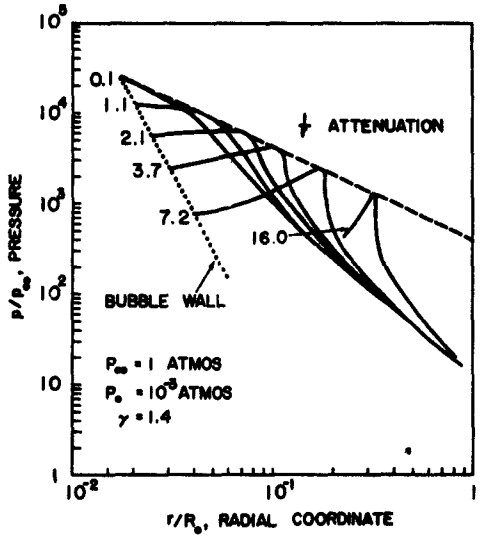

Fig. 5(b) Variation of pressure with distance from the bubble wall for different instants in time during the rebound of the bubble.

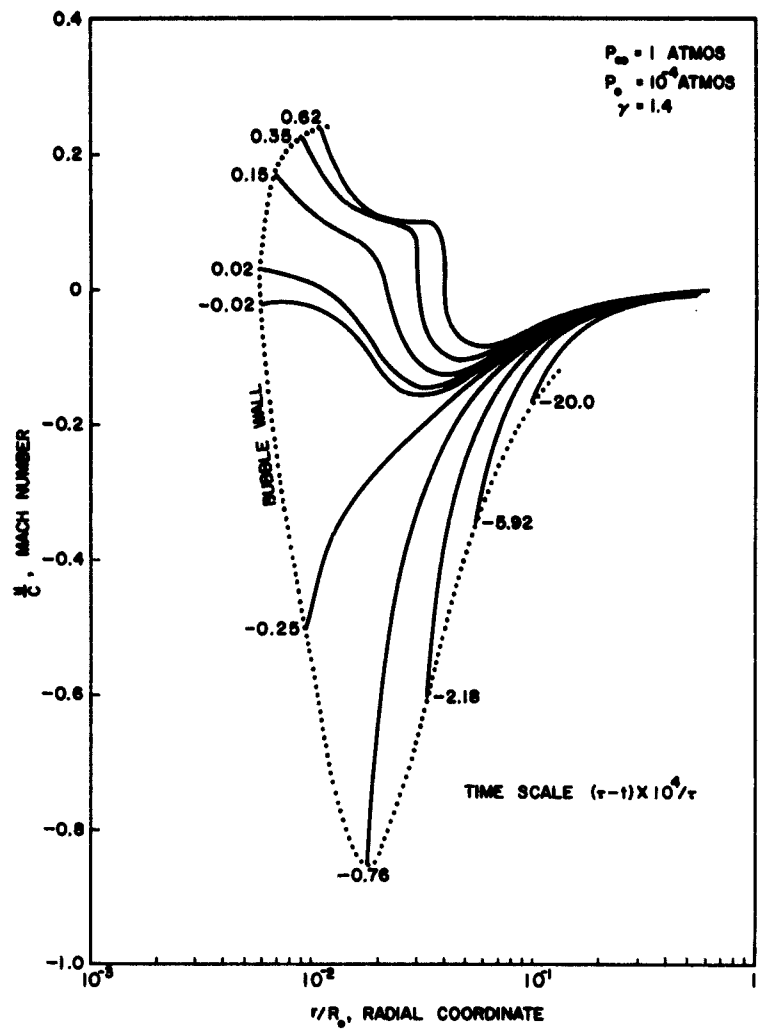

Fig. 6 Variation of Mach number with distance from the bubble wall for different instants in time during the collapse and rebound of the bubble. The initial pressure p_o in the gas is 10^{-4} atmospheres. The ambient pressure is 1 atmosphere.

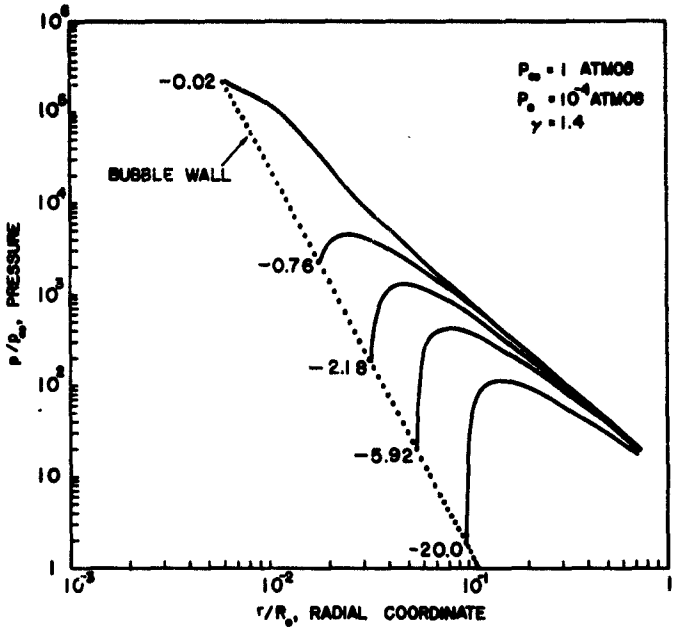

Fig. 7(a) Variation of pressure with distance from the bubble wall for different instants in time during the collapse of the bubble. The conditions correspond to those of Fig. 6.

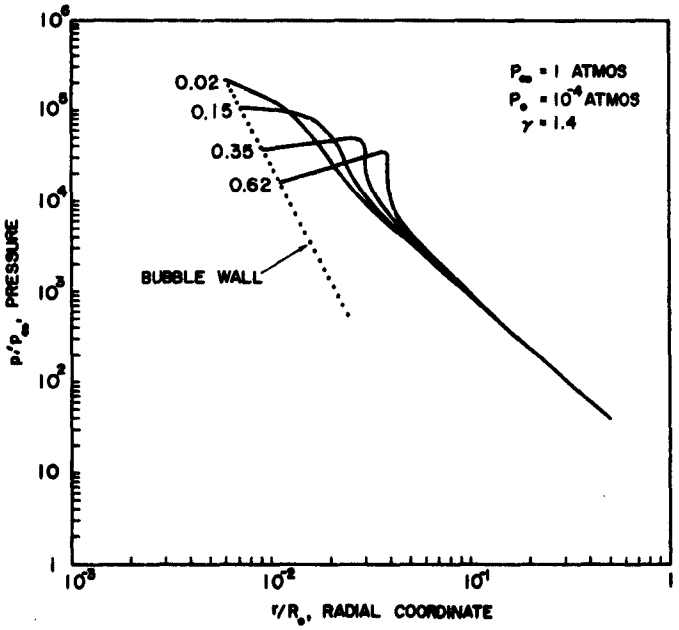

Fig. 7(b) Variation of pressure with distance from the bubble wall for different instants in time during the rebound of the bubble.

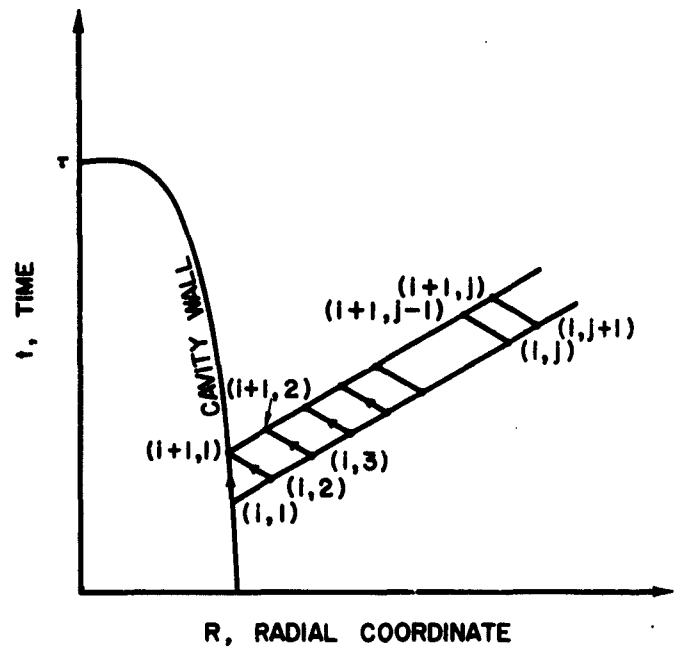

Fig. 8 Finite difference mesh in R - t plane for solution by method of characteristics.

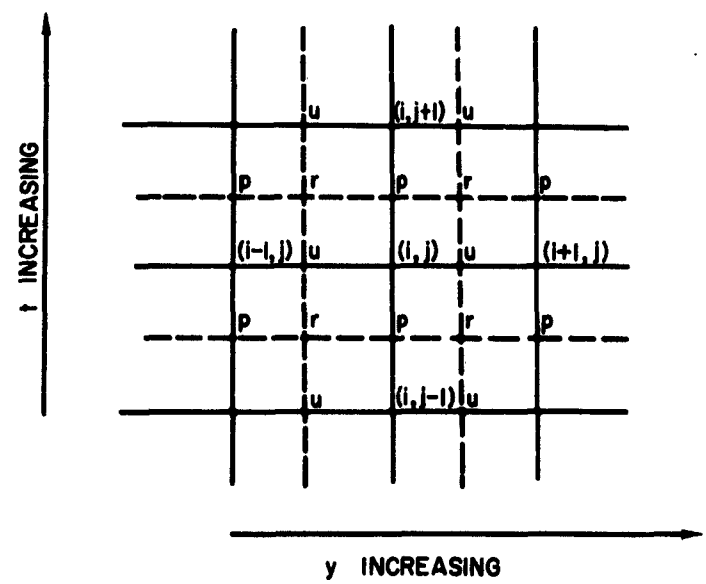

Fig. 9 Finite difference mesh in R - t plane for solution of Lagrangian equations.

DISTRIBUTION LIST FOR UNCLASSIFIED REPORTS ON CAVITATION

Contract Nonr-220(28)
Single Copies Unless Otherwise Given

Chief of Naval Research
Navy Department
Washington 25, D.C.
Attn: Code 438 (3)
Code 463

Commanding Officer
Office of Naval Research
Branch Office
The John Crerar Library Bldg.
Chicago 1, Ill.

Commanding Officer
Office of Naval Research
Branch Office
346 Broadway
New York 13, N. Y.

Commanding Officer
Office of Naval Research
Branch Office
1030 E. Green Street
Pasadena, California

Commanding Officer
Office of Naval Research
Navy 100, Fleet Post Office
New York, N. Y. (25)

Director
Naval Research Laboratory
Washington 25, D.C.
Attn: Code 2021 (6)

Chief, Bureau of Aeronautics
Navy Department
Washington 25, D.C.
Attn: Research Division
Aero and Hydro Branch
(Code Ad-3)
Appl. Mech. Branch
(Code DE-3)

Commander
Naval Ordnance Test Station
Inyokern, China Lake, Calif.
Attn: Technical Library

Commander
Naval Ordnance Test Station
3202 E. Foothill Blvd.
Pasadena, California
Attn: Head, Underwater Ord.
Head, Research Div.
Pasadena Annex Library

Chief, Bureau of Yards and
Docks, Navy Department
Washington 25, D.C.
Attn: Research Division

Chief, Bureau of Weapons
Navy Department
Washington 25, D.C.
Attn: Asst. Chief for Research
(Code Re)
Systems Director, Underwater Ord. (Code Rexc)
Armor, Bomb, Projectile, Rocket, Guided Missile Warhead and Ballistics Branch
(Code Re3)
Torpedo Branch(Code Re6)
Research and Components
Section (Code Re6a)
Mine Branch (Code Re7)

Chief, Bureau of Ships
Navy Department
Washington 25, D.C.
Attn: Research and
Development (Code 300)
Ship Design (Code 410)
Preliminary Design and Ship
Protection (Code 420)
Scientific, Structural and
Hydrodynamics (Code 442)
Submarine (Code 525)
Propellers and Shafting
(Code 554)

Commanding Officer and Dir.
David Taylor Model Basin
Washington 7, D.C.
Attn: Hydromechanics Lab.
Seaworthiness and Fluid
Dynamics Div.
Library

Commanding Officer
Naval Ordnance Laboratory
White Oak, Maryland
Attn: Underwater Ordnance Dept.

Commanding Officer
Naval Underwater Ordnance Sta.
Newport, Rhode Island

Director
Underwater Sound Laboratory
Fort Trumbull
New London, Conn.

Library
U.S. Naval Postgraduate Schl.
Monterey, California

Executive Secretary Research
and Development Board
Department of Defense
The Pentagon
Washington 25, D.C.

Chairman
Underseas Warfare Committee
National Research Council
2101 Constitution Avenue
Washington 25, D.C.

Director
National Bureau of Standards
Washington 25, D.C.
Attn: Fluid Mech. Section

Dr. G. H. Keulegan
National Hydraulic Laboratory
National Bureau of Standards
Washington 25, D.C.

Scientific and Technical
Information Facility
Attn: NASA Rep. (S/AK-DL)
P. O. Box 5700
Bethesda, Md.

Director
Langley Aeronautical Lab.
National Aeronautics and Space
Admin.
Langley Field, Virginia

Mr. J. B. Parkinson
Langley Aeronautical Lab.
National Aeronautics and
Space Administration
Langley Field, Virginia

Commander
Air Research and Development
Command
P. O. Box 1395
Baltimore 18, Maryland
Attn: Fluid Mechanics Div.

Director
Waterways Experiment Sta.
Box 631
Vicksburg, Mississippi

Beach Erosion Board
U.S. Army Corps of Engineers
Washington 25, D.C.

Office of Ordnance Research
Department of the Army
Washington 25, D.C.

Office of the Chief of Engineers
Department of the Army
Gravelly Point
Washington 25, D.C.

Commissioner
Bureau of Reclamation
Washington 25, D.C.

Director
Oak Ridge National Lab.
P. O. Box P
Oak Ridge, Tenn.

Sandia Corporation Library
Sandia Base
Albuquerque, New Mexico

Professor Carl Eckart
Scripps Institute of
Oceanography
La Jolla, California

Documents Service Center
Armed Services Technical
Information Agency
Arlington Hall Station
Arlington 12, Virginia (10)

Mr. A. B. Needham
Research Direction
Minneapolis Mining
Research Center
Minneapolis 17, Minn.

Office of Technical Services
Department of Commerce
Washington 25, D.C.

Division of Applied Mathematics
Brown University
Providence 12, Rhode Island

California Institute of Technology
Pasadena, California
Attn: Professor A. J. Acosta
Professor A. Hollander
Professor C. B. Millikan
Professor M. S. Plesset
Professor V. A. Vanoni
Professor T. Y. Wu

University of California
Department of Engineering
Berkeley 4, California
Attn: Professor H.A. Einstein
Professor H. A. Schade
Professor J. V. Wehausen

Case Institute of Technology
Department of Mechanical Eng.
Cleveland, Ohio
Attn: Professor G. Kuerti

Cornell University
Graduate School of Aero. Eng.
Ithaca, New York
Attn: Prof. W. R. Sears

Harvard University
Cambridge 38, Mass.
Attn: G. Birkhoff, Dept.
of Mathematics
G. Carrier, Div. of Eng. and
Applied Physics

University of Illinois
Dept. of Theoretical and
Applied Mechanics
College of Engineering
Urbana, Illinois
Attn: Dr. J. M. Robertson

State University of Iowa
Iowa Institute of Hydraulic
Research
Iowa City, Iowa
Attn: Dr. Hunter Rouse

University of Maryland
Inst. for Fluid Dynamics
and Applied Math.
College Park, Maryland
Attn: Prof. M. H. Martin
Prof. J. R. Weske

Massachusetts Inst. of Tech.
Cambridge 39, Mass.
Attn: Prof. W.M. Rohsenow
Dept. Mech. Engr.
Prof. A. T. Ippen, Hydro. Lab.

Michigan State College
Hydraulics Laboratory
East Lansing, Mich.
Attn: Prof. H.R. Henry

University of Michigan
Ann Arbor, Michigan
Attn: Director Engineer-
ing Institute
Prof. V. L. Streeter
Civil Eng. Dept.

University of Minnesota
St. Anthony Falls Hyd. Lab.
Minneapolis 14, Minn.
Attn: Dr. L. G. Straub

New York University
Inst. of Mathematical Sciences
25 Waverly Place
New York 3, New York
Attn: Prof. R. Courant

Dr. Th. von Karman
1051 So. Marengo Street
Pasadena, California

University of Notre Dame
College of Engineering
Notre Dame, Indiana
Attn: Dean K.E. Schoenherr

Pennsylvania State University
Ordnance Research Laboratory
University Park, Penn.
Attn: Prof. G.F. Wislicenus

Dr. J. Kotik
Technical Research Group
2 Aerial Way
Syosset, New York

Professor H. Cohen
IBM Research Center
P. O. Box 218
Yorktown Heights, New York

Stanford University
Stanford, California
Attn: Prof. D. Gilbarg
Dept. of Mathematics
Prof. L. I. Schoff
Dept. of Physics
Prof. J. K. Vennard
Dept. of Civil Engineering

Stevens Institute of Technology
Experimental Towing Tank
711 Hudson Street
Hoboken, New Jersey

Worcester Polytechnic Inst.
Alden Hydraulic Laboratory
Worcester, Mass.
Attn: Prof. J. L. Hooper

Aerojet General Corporation
6352 N. Irwindale Avenue
Asusa, California
Attn: Mr. C.A. Gongwer

Dr. J. J. Stoker
New York University
Inst. of Math. Sciences
25 Waverly Place
New York 3, New York

Professor C. C. Lin
Dept. of Mathematics
Massachusetts Inst. of Tech.
Cambridge 39, Mass.

Dr. Columbus Iselin
Woods Hole Oceanographic Inst.
Woods Hole, Mass.

Dr. A. B. Kinzel, Pres.
Union Carbide and Carbon
Research Laboratories, Inc.
30 E. 42nd Street
New York, N. Y.

Dr. F. E. Fox
Catholic University
Washington 17, D.C.

Dr. Immanuel Estermann
Office of Naval Research
Code 419
Navy Department
Washington 25, D.C.

Goodyear Aircraft Corporation
Akron 15, Ohio
Attn: Security Officer

Dr. F. V. Hunt
Director, Acoustics Research Laboratory
Harvard University
Cambridge, Mass.

Professor Robert Leonard
Dept. of Physics
University of California at Los Angeles
West Los Angeles, California

Technical Librarian
AVCO Manufacturing Corp.
2385 Revere Beach Parkway
Everett 49, Mass.

Dr. L. Landweber
Iowa Inst. of Hydraulic Research
State University of Iowa
Iowa City, Iowa

Dr. M. L. Ghai, Supervisor
Heat Transfer/Fluid Mechanics
Rocket Engine-Applied Res.
Building 600
Aircraft Gas Turbine Div.
General Electric Co.
Cincinnati 15, Ohio

Dr. W. W. Clauson
Rose Polytechnic Institute
R.R. No. 5
Terre Haute, Indiana

Mr. Kurt Berman
Rocket Engine Section
Aircraft Gas Turbine
Development Department
Malta Test Station
Ballston Spa, New York

Officer in Charge
MWDP Contract Supervisory Staff
SACLANT ASW Research Center
APO 19, New York, N. Y.

Hydronautics, Inc.
Pindell School Rd., Howard County
Laurel, Maryland
Attn: Mr. Phillip Eisenberg
Mr. Marshall Tulin

Commanding Officer and Dir.
U. S. Naval Civil Eng. Lab.
Port Hueneme, California
Attn: Code L54

Dr. H. L. Uppal, Director
Irrigation and Power Res. Inst.
Punjab, Amritsar, India

Prof. Taizo Hayashi, Director
Hydraulics Laboratory
Chuo University
1, 1-chome, Koishikawamati
Bunkyo-ku, Tokyo, Japan

Prof. J. E. Cermak
Dept. of Civil Engineering
Colorado State University
Fort Collins, Colorado

Mr. John P. Herling
Order Librarian
Engineering Societies Library
United Eng. Trustees, Inc.
29 West 39th Street
New York 18, N. Y.

Mr. R. W. Kermeen
Dept. 8173, Bldg. 102
Lockheed Missile and Space Company
P. O. Box 504
Sunnyvale, California

Material Laboratory Library
Building 291, Code 912B
New York Naval Shipyard
Brooklyn 1, New York

Prof. Frederick G. Hammitt
Nuclear Engineering Dept.
The University of Michigan Research Institute
Ann Arbor, Michigan

Commanding Officer
NROTC and Naval Adm. Unit
Massachusetts Inst. of Tech.
Cambridge 39, Mass.

Commanding Officer and Dir.
U.S. Navy Mine Defense Lab.
Panama City, Florida